

The 6.7 keV thermal emission lines in the stellar flare spectra of two chromospherically active Binaries: Algol and GT Mus

Ambrose Chukwudi Eze^{a,b,*}, Sudum Esaenwi^c, Fidelis Okey Madu^a

^a Department of Physical and Geosciences, Godfrey Okoye University, Enugu State, Nigeria

^b Department of Physics and Astronomy, University of Nigeria, Nsukka, Nigeria

^c Department of Physics, Rivers State University, Port Harcourt, Nigeria

Received 16 February 2021; received in revised form 25 September 2021; accepted 30 September 2021

Available online 8 October 2021

Abstract

Chromospherically active binaries' (CABs) are late-type evolved stars with strong chromosphere/corona and high flare activity levels. Starspot evolution in these CABs and binaries reveals strong stellar and chromospheric activities. In binaries, the tidal interaction via the internal dynamo motion, during rapid rotation of the component stars generates magnetic fields. The magnetic activity heats the tenuous coronal plasma, and the reconnection of energetic particles leads to stellar flare formation. Cyclic-variation signatures in brightness and emission lines are indicators of coronal/chromospheric activities. The spatial population densities of CABs are large, and their hard energy spectral characteristics are prominent in our galaxy. Photo-ionization/collisional excitation processes in the corona of CABs generate a strong thermal emission line at 6.7 keV. In the present work, we re-analyzed stellar flare data of two CABs (Algol & GT Muscae) observed with Suzaku. We resolved the 6.7 keV emission spectrum and equivalent width (EW) in each source's stellar flare data. The resolved energy spectra are remarkably similar to that of the hard energy spectra at 6.7 keV of X-ray point sources observed in different Galactic regions. The EW of the 6.7 keV emission line obtained in this work compares favorably with the EW range (260 eV – 980 eV) of the 6.7 keV energy spectra of Galactic point sources. Hence, cumulative X-ray emission lines of coronal plasma (and their EWs) emitted by numerous point sources in different Galactic plane positions give clues on the Galactic Ridge X-ray Emission (GRXE) mechanism. We are of the view that CABs could account for a large number of fast-transient X-ray sources that emit thermal emission line at 6.7 keV during their quiescent and flared phases, and these underlying population sources could contribute significantly to the total luminosity of 6.7 keV GRXE.

© 2021 COSPAR. Published by Elsevier B.V. All rights reserved.

Keywords: Flare-stars; Active stars; Binaries; Chromospheric activity; Corona; Stellar flares; X-ray; GRXE

1. Introduction

Chromospherically active binaries (CABs) are magnetically active stars with large convection zones/envelopes. They are often referred to as members of binaries though some single stars are included. CABs are spectral class F to M in the H-R diagram and most eclipsing detached-,

and semi-detached-binary systems belong to these spectral classes. The component stars of the system orbit one another around their common barycenter. CABs exhibit strong coronal/chromospheric activity levels as well as a transition region (Strassmeier et al., 1988, Pettersen, 1989; Dempsey et al., 1993; Demircan et al., 2006). CABs are grouped in terms of Solar mass abundance; sub-giants stars ($2.5 - 5 M_{\odot}$), main-sequence stars ($<1.7 M_{\odot}$), and evolved stars ($\sim 1.4 M_{\odot}$) respectively (Barrado et al., 1994, 1997). CABs are further classified according to their evolutionary stages; main-sequence stars, top red-giant

* Corresponding author at: Department of Physical and Geosciences, Godfrey Okoye University, Enugu State, Nigeria.

E-mail address: jerry410001@gmail.com (A.C. Eze).

branch stars (T-RGB stars), bottom red-giant branch stars (B-RGB stars), evolving off main-sequence stars (E-off MS stars), and stars on the horizontal branch. This classification has been affirmed and the nomenclature used in the classification excludes RR Lyrae stars on the horizontal branch (Barrado et al., 1998). Previous studies have revealed the stellar properties of the component stars (e.g. Strassmeier et al., 1993; Dempsey et al., 1993; Eker et al., 2008). One component of the system is a donor star which should be in proximity with the companion. The outflow of matter from the surface of the donor star accretes onto the companion (accretor) during rapid and synchronous rotation. Roche Lobe overflow and/or stellar wind mechanisms explain the physical process behind the mass accretion in these binary systems. Among all the CABs, it is only RS CVn and BY Draconis binary systems that do not undergo a mass accretion process (Barrado et al., 1998). Generally, the stellar properties of numerous CABs are vital tools for studying the stellar structure as well as testing the stellar evolution models (Barrado et al., 1994, 1998; Montes et al., 1999). Rapid and synchronous rotation of the component stars is sustained by the tidal interaction (Eker et al., 2008). The stellar dynamo mechanism generates a strong magnetic field in the coronae (Galvez et al., 2009). Magnetic coupling triggers intense churning and re-connection of energetic particles. Sudden and rapid eruptions of energy release and relaxation (processes of the magnetic field) in the coronae are indications of stellar flares, and these happen on time scales of hours to days.

Geometric effects and rotational modulations are caused by starspots. Starspot evolution in CABs hints more coronal/chromospheric activity than in the normal single stars of the same mass and evolutionary stage for a given effective temperature (e.g. Montes et al., 1996a; Zhao et al., 2011, 2013). Therefore, starspots are responsible for periodic variations in surface brightness. Some CABs exhibit long-duration cyclic variations in brightness whereas others exhibit short-duration cyclic variations. These are as a result of changes in the activity structure of starspot on timescales of hours to days, sometimes in months to years depending on magnetic activities (O'Neal et al., 1998a, b; O'Neal, 2006).

The flare emission measure depends on temperature. An increase in temperature leads to large emission measures and perhaps emission lines of chemical abundances, and X-ray flux variability (White et al., 1980; Garcia et al., 1980; Barrado et al., 1998; Drake, 2003a). These emission lines are indicators of chromospheric activity from turbulent mixing of energetic particles/plasma induced by magnetic field coupling in the convective zones (Covino et al., 2001; Morel et al., 2003; Gudel, 2004). Chromospheric activity varies with the rotation velocity, which in turn influence the dynamo mechanism. Thus, fast rotation velocity enhances stellar flare activities/chromospheric emissions (Montes et al., 2000, 2001a; Audard et al., 2003; Zhang et al., 2015). Variable H α , Ca II H and K

emission features, photometric variations, X-ray emission, and other spectral lines of chemical abundance are good characteristics/indicators of strong coronal/chromospheric activities (e.g. Montes et al., 1996a; O'Neal et al., 1998a; Cao, & Gu, 2015).

Intensity of chromospheric emissions depends on the “degree” of the stellar activity level, and it originates mostly from the magnetic activities of the donor stars in the system (White et al., 1980; Garcia et al., 1980). This suggests that the convective zone depth and luminosity class of magnetically active donor stars are greater than that of the companion (Montes et al., 1998; Biazzo et al., 2007). These have been affirmed spectroscopically and photometrically (e.g. Strassmeier et al., 1993; Bleach et al., 2002). However, the contribution of the companion star might not be negligible. In some CABs, both components of the binary system contribute significantly to the radiative flux observed in multi-wavelengths (Berdyugina, 2005).

Flare activities of CABs are enormous and X-ray radiation is emitted in the process (Garcia et al., 1980; Benz and Guedel, 1994). It is widely believed that X-ray emission from astrophysical sources traces magnetic activities (Nordon & Behar, 2007; Clarke et al., 2018). These characteristics depend on the stellar flare and coronal/chromospheric activity level of the underlying populations. The population densities of about 10^{-5} to 10^{-3} pc $^{-3}$ for CABs within 25 – 200 parsec of the Galactic plane have been inferred (Favata et al., 1995; Warwick, 2014). Moreover, 65% – 80% of the Milky Way stellar population density is occupied by dwarf stars and binaries. About 75% of these dwarfs exhibit strong stellar flare activities accompanied by X-ray emission (Yoldas, & Dal, 2017). These dwarfs are in chromospherically active binaries, and numerous CABs have been observed in our galaxy (e.g. Strassmeier et al., 1988, 1993; Demircan et al., 2006; Eker et al., 2008). These sources could account for a large number of X-ray fast-transients (Montes et al., 1998) that emit thermal emission line at 6.7 keV during their quiescent and flared phases (Warwick, 2014). To this end, Algol and GT Muscae are chromospheric X-ray active binaries. Algol and GT Muscae are among the transient and variable flare star candidates with a typical cyclic-variation signature in brightness. Photo-ionization or collisional excitation processes in the corona of variable flare stars, active stars, and binaries with intrinsic X-ray luminosity range; 10^{30-34} ergs $^{-1}$ generate strong thermal emission line at 6.7 keV (Matsuoka et al., 2011; Warwick, 2014; Xu et al., 2016; Tsuboi et al., 2016).

1.1. Algol

Algol is a triple hierarchical extrinsic variable system containing B-, K- and F-type stars (Baron et al., 2012). It is located in the constellation Perseus at a distance of about ~ 28 parsecs (Antunes et al., 1994). The mass of the trio is 3.7 M_{\odot} , 0.81 M_{\odot} , and 1.6 M_{\odot} respectively (Favata, & Schmitt, 1999; Zavala et al., 2010). The B-

and K-stars are the inner eclipsing binary system and they are orbited by the more distant F-star (outer orbit). Photometric observations of the shallow eclipse revealed that the inner orbit (orbit of B-K-stars) and outer orbit (orbit of B-K-stars and F-star) of the system are perpendicular (Söderhjelm, 1980). But whether the orbits (inner and outer) exhibit prograde or retrograde rotations was not certain. Lestrade et al. (1993) were of the view that the inner orbit of the system has a retrograde movement whereas the outer orbit is prograde. However, Csizmadia et al. (2009) reported that the inner orbit of the system exhibits prograde rotation whereas the outer orbit is retrograde. This conflict was resolved by the optical investigation of the orbital motion of the system; thus, the inner and outer orbit exhibit retrograde and prograde movement respectively (Zavala et al., 2010). These have been supported by the Very Long Baseline Interferometer (VLBI) astrometric study (Peterson et al., 2011).

This anomaly in the rotational movements of the inner and outer orbits suggests that the F-star might have a negligible role in the mass accretion processes observed in the Algol binary system. Moreover, the F-star likely not a rapid rotator since it takes about 680 days (~ 1.86 years) to revolve around the inner pair stars whose orbital period is 2.867 days (Zavala et al., 2010; Baron et al., 2012). This also suggests that the F-star has no significant contribution to the activity-cycle variations in brightness and/or X-ray emission. Given this, the F-star is not taken into consideration while studying the X-ray emission of Algol (e.g. Schnopper et al., 1976; Stern et al., 1992; Ottmann, & Schmitt, 1996). Therefore, our discussion follows suit. The inner pair stars (B- and K-star) are tidally locked semi-detached binary system with an angle of inclination, and binary separation of about 81.4° , and $14.14 R_\odot$ respectively ($R_\odot = 6.957 \times 10^5$ m; Favata & Schmitt, 1999; Eze, A., et al., 2017). The B-star is a main-sequence star whereas the K-star is a late-type sub-giant. The B-star is supposed to be a sub-giant star since it is more massive than its companion in accord with the stellar evolution model. However, several observations of Algol revealed that the reverse is the case. This inconsistency is called the “Algol paradox” (Favata & Schmitt, 1999). Ab initio, the K-star was initially the more massive component star of the system and evolved more rapidly than the B-star. The tidal interaction between the component stars during rapid rotation triggered the magnetic dynamo process. This in turn channels accretion of matter from the Roche-lobe-filling K-star via the inner Lagrangian point onto the B-star. The mass accretion is driven either by the expansion of the K-star or the shrinking of binary separation due to angular momentum loss. Therefore, mass transfer changed the mass ratio. Hence, the B-star becomes more massive (Favata, & Schmitt, 1999; Yang et al., 2011). For detailed stellar properties and extensive studies on Algol (see; Pallavicini et al., 1981; Richards, 1993), and reference therein.

1.2. GT Muscae

GT Muscae (GT Mus), is a bright spectroscopic quadruple containing a detached binary system. It is located eastwards in the constellation Musca at Right Ascension and Declination ($11^{\text{h}} 39^{\text{m}} 29.63^{\text{s}}$ and $-65^\circ 23' 51.9''$), and at a distance; ~ 501 light-years. GT Mus exhibits chromospheric chemical abundance and Ca II, H, K and variable H α emission (Collier, 1987; Pallavicini et al., 1992; Murdoch et al., 1995) as well as strong X-ray emission maintained by intense starspot and flare activities (Garcia et al., 1980). GT Mus consists of single-lined RS Canum Venaticorum (RS CVn) of G5/8III and its companion pair of eclipsing A0/2V spectral type stars (Hearnshaw et al., 2012). Previous observations of GT Mus reveal that it has a long orbital period of about 64.3 days shared among the components stars; RS CVn-star has orbital period of 61.52 days whereas that of the eclipsing binary is 2.75 days. The component stars orbit one another, and their binary separation is about 0.23 arc-seconds. In the Hipparcos catalogue, RS CVn is an active late-type star, designated as HD 101379, whereas the eclipsing star is HD 101380 (Hall, 1976). GT Mus exhibits starspots, chromospheric activity with low amplitude quasi-sinusoidal light curve variations. That is, GT Mus exhibit short-period variability in magnitude (Murdoch et al., 1995). The activity-cycle variations in brightness are due to starspot evolution (Jones et al., 1995; Hearnshaw et al., 2012). The photometric variability and spectral geometry of GT Mus are attributed to the starspots activity-cycle and rotation of the RS CVn respectively. This suggests that the chromospheric/stellar activity and X-ray emission originates from the corona of RS CVn (Dempsey et al., 1993).

Mass accretion has not been observed in GT Mus (Barrado et al., 1994, 1997, 1998). Also, stellar characteristics such as a large convective envelope, coronal activity, transition region, coronae, and strong chromospheric emission have been inferred. This confirmed that GT Mus is a chromospherically active star (Demircan et al., 2006). Details of the stellar properties and photometric analysis of GT Mus can be found in the following work (see; Murdoch et al., 1995; Hearnshaw et al., 2012), and reference therein.

1.3. X-ray observations of Algol and GT Mus

Magnetic reconnection on a surface of active stars and binaries is accompanied by sudden energy release and relaxations; thus, stellar flare formation. Energetic X-ray stellar flares activities on the surface of Algol and GT Mus have been observed by different X-ray missions.

Algol was first detected as a variable X-ray source with SAS- 3 in October 1975 (Schnopper et al., 1976). Later in December 1975, an X-ray telescope aboard Aerobee 350 rocket flight confirm that Algol is a strong X-ray emitter with an order of magnitude in variability and mass transfer

via the Roche Lobe overflow mechanism explain the X-ray emission (Harden et al., 1977). Algol exhibit strong chromospheric and starspot activities and SSS (Solid State Spectrometer) onboard Einstein Observatory (High Energy Astronomy Observatories-2) inferred sporadic flaring episodes with the rapid rise and decay in brightness on time-scales of 12 h, and the X-ray emission originates from the active corona surrounding the donor star (White et al., 1980). Evidence of flaring activities in Algol was bolstered by EXOSAT (European X-ray Observatory SATellite) observation which inferred sporadic large stellar flares (White et al., 1986). This was supported by GINGA's (Japanese for 'galaxy') observation that Algol's stellar flares are characterized as "two-ribbon" long-duration giant flares with the presence of Fe abundance in the convection zone (chromospheres/coronal) during the quiescent and flared epochs. The two-ribbon flares manifest as a gradual slow rise to the peak and then decay of magnetic/stellar activities. The signature of the variation in brightness during the epochs depicts the X-ray light curve.

Previous spectroscopic and photometric studies on Algol have revealed the chromospheric activities and other physical parameters of the system (Reference therein). Hydrogen column density (N_H) variations during the quiescent and flaring epochs of Algol have been revealed by ROSAT (Röntgen Satellite) observation. The spectral result of stellar flare data modeled with a two-temperature thermal model shows that N_H in the corona around the B-type star varies in the range; $(3.2 - 12) \times 10^{19} \text{ cm}^{-2}$ at different orbital phases. The first and second thermal temperature of the plasma and that of the emission measure (EM) varies in the range; $(1.9 - 2.4) \times 10^6 \text{ K}$ and $(1.4 - 2.3) \times 10^7 \text{ K}$ and $(0.6 - 1.4) \times 10^{53} \text{ cm}^{-3}$ and $(3.2 - 10) \times 10^{53} \text{ cm}^{-3}$ respectively. The variations of N_H suggests that the accretion around the B-type star is optically thin. Moreover, particle recombination (due to magnetic activities and/or reconnection) heat different layers of the corona (coronal heating) which in-turn causes variations in temperature and emission measure at different orbital phases. Therefore, changes in the emission measures are responsible for the X-ray flux variability (Ottmann, 1994). Singh, Drake & White, (1995) used thermal plasma emission models (single-, two- and three-component; T vmekal, 2 T vmekal, 3 T vmekal) to fit the X-ray stellar flare data of Algol observed with ASCA and ROSAT in the, 2 – 3 keV, 0.6 – 0.7 keV and 0.2 – 0.3 keV energy bands respectively and reported variations in the emission measures (EM), temperature and hydrogen column density. The value of the obtained individual physical parameter is in the range; $(1.7 - 5.8) \times 10^{53} \text{ cm}^{-3}$, 0.18 – 2.70 keV, and $(3.1 - 3.7) \times 10^{19} \text{ cm}^{-2}$ respectively. This suggests that the two- and three-component thermal plasma emission models better fit the data in the lower energy bands. However, authors were of the view that excess absorption due to circumstellar material and/or presence of unresolved soft X-ray emission could cause a low value of hydrogen column densities in Algol when

compared to that of the standard value $\sim 10^{22} \text{ cm}^{-2}$. Moreover, the low value of N_H could also be due to the presence of cool gas surrounding the chromospheric active K-star (Yang et al., 2011). XMM-Newton observation inferred a variation in the value of hydrogen column density (N_H) during the quiescent and flared epochs of Algol. The value of N_H during the quiescent and flared epochs varies from $2.19 \times 10^{20} \text{ cm}^{-2}$ to $2.81 \times 10^{20} \text{ cm}^{-2}$ (Yang et al., 2011). Yang et al. fitted Algol's quiescent and flared data with a two-component thermal emission model (2 T vmekal) using XSPEC in the 0.3 keV – 8 keV energy bands. The authors resolved 6.7 keV line in the X-ray spectrum and constrained the temperature of $(2.0 - 3.7) \times 10^7 \text{ K}$ and $(5.8 - 6.9) \times 10^6 \text{ K}$ during the flared and quiescent epochs respectively. The X-ray flux, emission measures (EM), and reduced Chi-squared value during the flared and quiescent epochs vary from $(4.49 - 16.1) \times 10^{-11} \text{ erg cm}^{-2}\text{s}^{-1}$, $(4.59 - 12.48) \times 10^{53} \text{ cm}^{-3}$, 1.50 – 1.71 respectively. The authors later re-fitted the X-ray spectrum with a three-component thermal emission model (3 T vmekal) and obtained an improved reduced Chi-squared value in the range 1.36 to 1.52 during the quiescent and flared epochs. Observations of Algol with ROSAT, EXOSAT, Chandra, and XMM-Newton show that the high and low temperature in the stellar flares during quiescent and flared epochs are co-spatial with the size of their scale height comparable to that of the stellar radius (Ottmann, 1994; reference therein). This suggests that there are different layers of the extended corona around the K-type star and/or the stellar surface of the system have preflare heating (Favata et al., 2000). The size and location of the flaring region around the south polar region and/or on the "northern" hemisphere of the K-type star have been constrained using BeppoSAX and XMM-Newton observed stellar flare data (e.g. Ottmann, 1994; Schmitt & Favata, 1999; Schmitt, Ness, and Franco, 2003; Sanz-Forcada, Favata, & Micela, 2007).

On the other hand, the light curve of GT Mus is characterized by low amplitude quasi-periodic variation in brightness. Modeling the stellar flare data of GT Mus with optically thin thermal plasma (mekal and apec) and absorption (Tbabs) models to fit the spectra in the 2 – 10 keV energy bands revealed hydrogen column density (interstellar absorption) of $(4.2 - 5.9) \times 10^{20} \text{ cm}^{-2}$ respectively. Physical parameters such as temperature, luminosity, and emission measures in the range 4 – 11 keV, $(2 - 5) \times 10^{33} \text{ erg s}^{-1}$ and $(7 - 23) \times 10^{55} \text{ cm}^{-3}$ respectively have been constrained from eight years observation of GT Mus with Monitor of All-sky X-ray Image (MAXI) and Neutron star Interior Composition Explorer (NICER; Schmitt & Favata, 1999; Tsuboi et al., 2016; Sasaki et al., 2021). Moreover, a spectral study revealed that stellar flare of GT Mus radiates an energy of about $(3 - 16) \times 10^{37} \text{ erg}$ and $(9 - 73) \times 10^{37} \text{ erg}$ during the flared and decay epochs that lasted for 2 – 6 days and 1 – 4 days respectively (Tsuboi et al., 2017; Sasaki et al., 2021).

MAXI observations of active stars and binaries (e.g. dMe stars, Algol, GT Mus, Young Stellar Objects) revealed

that the stellar flares of these systems radiates energy of about 10^{34-39} ergs and their X-ray luminosity and emission measure in the 2 – 20 keV band is 10^{31-34} ergs s⁻¹, and 10^{54-57} cm⁻³ respectively (Tsuboi et al., 2016, 2017).

The activity-cycle variations in these two chromospherically active binaries (Algol and GT Mus) are due to star-spot evolution though the cause of variations in the element abundance is not ascertained (Stern et al., 1992; Jones et al., 1995; Hearnshaw et al., 2012). Einstein and EXOSAT observations inferred that all late-type stars and binaries possess strong coronal and chromospheric activities during their rapid rotation and this process involves the conversion of magnetic energy to coronal X-ray emission. Moreover, ROSAT all-sky survey/observations of active binaries have revealed the stellar properties of Algol-type and RS CVn systems (Dempsey et al., 1993; Demircan et al., 2006). The X-ray emission of Algol and GT Mus is characterized by significant stellar/chromospheric and flaring activities in the coronae, and these have been confirmed by different X-ray missions; Einstein, GINGA, EXOSAT, ASCA, and ROSAT (e.g. Garcia et al., 1980; Favata & Schmitt, 1999). Evidence of more element abundances (N, O, Ne, Mg, Si, S, Ar, Ca, Fe, Ni), and Fe K–line at 6.7 keV in the quiescent and flared epochs have been reported from the stellar flare data of Algol and GT Mus observed by Einstein, ASCA, ROSAT, and Suzaku (Garcia et al., 1980; Antunes et al., 1994; Singh, Drake & White, 1995; White, 1996; Xu et al., 2016). Variation of element abundance during the evolution of stellar flares is believed to be a result of the chromospheric evaporation process and this has been confirmed by different X-ray missions (e.g. GINGA, ROSAT, BeppoSAX; Stern et al., 1992; Ottmann & Schmitt, 1996; Favata & Schmitt, 1999; Tsuboi et al., 2016; Sasaki et al., 2021). Moreover, the X-ray emission from Algol and GT Mus is a result of intense starspots and flaring activities in the corona of the active giant or sub-giant component stars of the system. In other words, the bulk of the X-ray emissions from Algol and GT Mus originates from the coronal/magnetic activities of the Roche lobe-filling secondary K-star and RS CVn component star respectively. Thence, an increase in coronal/flares activities results in a corresponding increase in coronal temperature, emission measure, and X-ray emission (Ottmann, 1994; Singh et al., 1996). This has been confirmed by different X-ray missions; Einstein, GINGA, EXOSAT, ROSAT, ASCA, Chandra, and XMM-Newton (White et al., 1980; Garcia et al., 1980; Favata et al., 2000; Schmitt, et al., 2003; Chung et al., 2004; Nordon and Behar, 2007). Fe K complex line in the X-ray spectrum resolved from Algol's stellar flare data observed with BeppoSAX & XMM-Newton has been reported, but the equivalent width of the complex line emission was not inferred (Favata & Schmitt, 1999). Also, high Fe abundant at the 6.7 keV line emission during the quiescent and flared epochs observed by the XMM-Newton have been inferred, but the equivalent width of the 6.7 keV line emission was not reported (Yang et al.,

2011). Eze A. et al. (2017) fitted the X-ray stellar flare data of Algol in the 4.5 – 7.5 keV energy bands and resolved 6.7 emission line in the stellar flare data of Algol and equivalent width of 510 eV. Also, GT Mus is an RS CVn-type system, and observations of Algol and GT Mus by MAXI/GSC have reported intense large stellar flares activities with luminosity; $10^{31} - 10^{34}$ ergs⁻¹ in the 2 – 20 keV, but 6.7 keV line emission was not resolved in the sources' spectra (Tsuboi et al., 2016). Xu et al. (2016) fitted the stellar flare data of GT Mus with the optically thin thermal plasma model (apec) in the 5 – 10 keV energy bands and resolved 6.7 emission line in the stellar flare data of GT Mus with an equivalent width of 259 eV.

All these X-ray missions/observations yielded significant contributions on the tidally-induced coronal/chromospheric activities and X-ray emission of these two chromospherically active binaries. Suzaku's spectrometers have a high resolution when compared to other X-ray missions operated in the 0.3 – 10 keV bands (Xu et al., 2016), and its observations affirmed the stellar flare activities/brightness of Algol is a two-ribbon flares type whereas that of GT Mus is quasi-periodic short-cyclic. Variable active stars and binaries with intense flare episodes and X-ray luminosity; 10^{30-34} ergs⁻¹ emit thermal emission line at 6.7 keV (reference therein). The 6.7 keV emission line is an intense emission iron feature believed to originate from discrete sources along the Galactic ridge, and the probable candidate sources include RS CVn systems, white dwarf stars, and coronally-active stars and binaries (Koyama et al., 1986). Einstein, EXOSAT, and ROSAT observations of X-ray emitters attributed the 6.7 keV line

emission to the thermal emission in the coronae (Singh et al., 1996). Spectral analysis of Fe K complex line at 6.7 keV and its equivalent width in the stellar flare data of Algol and GT Mus observed by Suzaku has been reported (Eze R. et al., 2015b; Xu et al., 2016; Eze A. et al., 2017; Goodwill et al., 2019). Chandra, XMM-Newton, Suzaku, and other X-ray missions provided a wealth of information on the underlying Galactic population discrete/point sources. As a result, comprehensive knowledge on surface brightness distribution and spectral properties of the Galactic Ridge X-ray Emission (GRXE) along the Galactic plane have been revealed. GRXE is an integrated X-ray emission from Galactic point sources (e.g. Ebisawa et al., 2008; Yamauchi et al., 2009; Uchiyama et al., 2013; Warwick, 2014).

1.4. Galactic Fe K α -line X-ray emission

Flaring activities in CABs are due to the active nature of large stellar spots and deep convection zones. Magnetohydrodynamic processes generate high levels of coronal activities and intense magnetic fields that transport energetic particles. The recombination of these particles by magnetic activities/reconnection leads to stellar flare formation. The chromospheric emission observed in CABs depends on the stellar flare activity level (Drake et al.,

1997; Garcia-Alvarez et al., 2009; Testa et al., 2015). Active stars of spectral class F to M are X-ray sources (Gudel, 2004; Berdyugina, 2005; Pye et al., 2015). These sources show a wide range of X-ray coronal emission of several orders of magnitude (Benz and Guedel, 1994; Drake et al., 2000). Fe $K\alpha$ - emission is one of the indicators of strong coronal/chromospheric activities associated with acceleration of electrons (Garcia et al., 1980; White et al., 1980; Testa, 2010). Fe $K\alpha$ -emission has prominent features at 6.4 keV, 6.7 keV, and 7.0 keV. These energies are observed as X-ray emission lines in the Galactic ridge; Galactic Ridge X-ray Emission (GRXE; Ebisawa et al., 2008; Revnivtsev et al., 2009).

Therefore, emission line energy and its widths give clues about the GRXE mechanism (Ebisawa et al., 2008). The 6.7 keV and 7.0 keV are thermal emission lines while 6.4 keV is the fluorescence emission line in nature. The 6.4 keV emission line originates from the reflection of incident X-rays by cold gas (Yuasa et al., 2010; 2012). The 6.7 keV and 7.0 keV GRXE are due to photo-ionization/collisional excitation processes in the vicinity of numerous discrete coronally X-ray sources (Eze et al., 2015b, 2017; Revnivtsev et al., 2009). The characteristic plasma temperature that generates 6.7 keV and 7.0 keV photon-counts/fluxes in the corona of Galactic point sources is 3 – 7 keV (Warwick, 2014). For plasma temperature of $3 < kT < 5$ keV, the photon-count/fluxes of 6.7 keV become prominent and surpass that of the 7.0 keV, but when the temperature of the coronal plasma is enhanced to 5 – 7 keV, the photon-count/fluxes of 7.0 keV become prominent (Warwick, 2014). GRXE is a measure of the cumulative emission of numerous Galactic X-ray emitters. In other words, GRXE originates from the integrated X-ray emissions of Galactic point sources. The spatial variations of GRXE properties in the Galactic plane are indications of variations in the stellar mass populations (e.g. Krivonos et al., 2007; Revnivtsev et al., 2009; Yamauchi et al., 2009). Plausible candidate sources of GRXE have been reported with active stars and binaries are inclusive. Algol and GT Mus are coronally active binaries (Matsuoka et al., 2011; Warwick, 2014; Tsuboi et al., 2016; Xu et al., 2016).

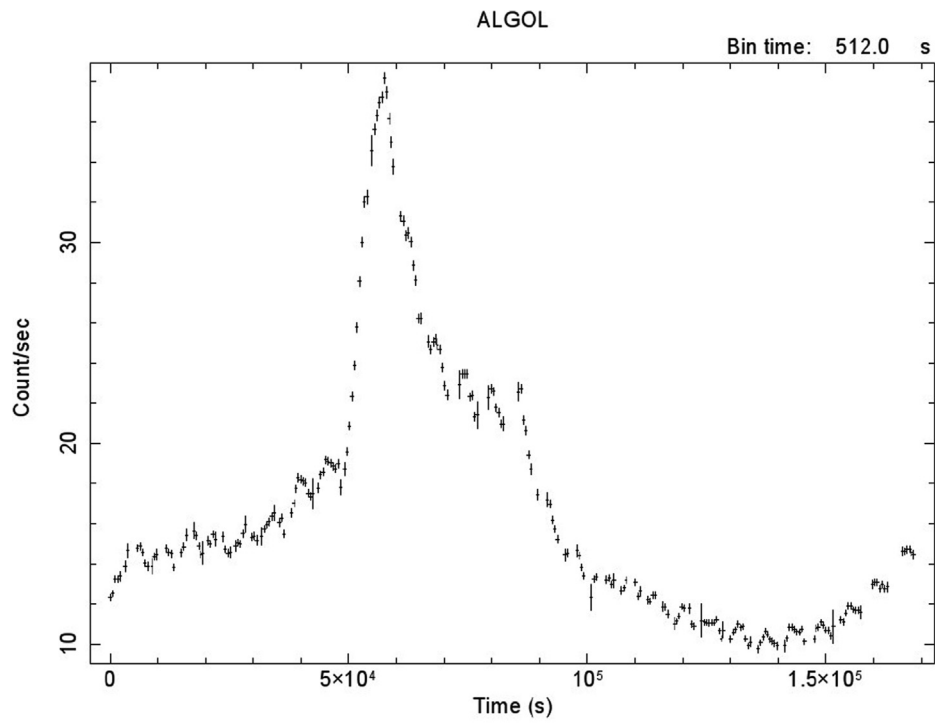
In this present work, we concentrated on the thermal emission line at 6.7 keV. Analysis of the sources' data is described in § 2. The results of the analysis are presented in § 3. Discussion of results and conclusion are presented in § 4 and § 5 respectively.

2. Data acquisition and analysis

We retrieved the stellar flare photon count/flux of the individual source from the Suzaku public archive. Algol and GT Mus were observed by the X-ray Imaging Spectrometer (XIS) of the X-ray telescope (XRT) on-board Suzaku satellite on March 8th, 2007 (Obs Id: 401093010), and December 12th, 2007 (Obs Id: 402095010) for 170 ks and 230 ks exposure respectively. Suzaku satellite has a

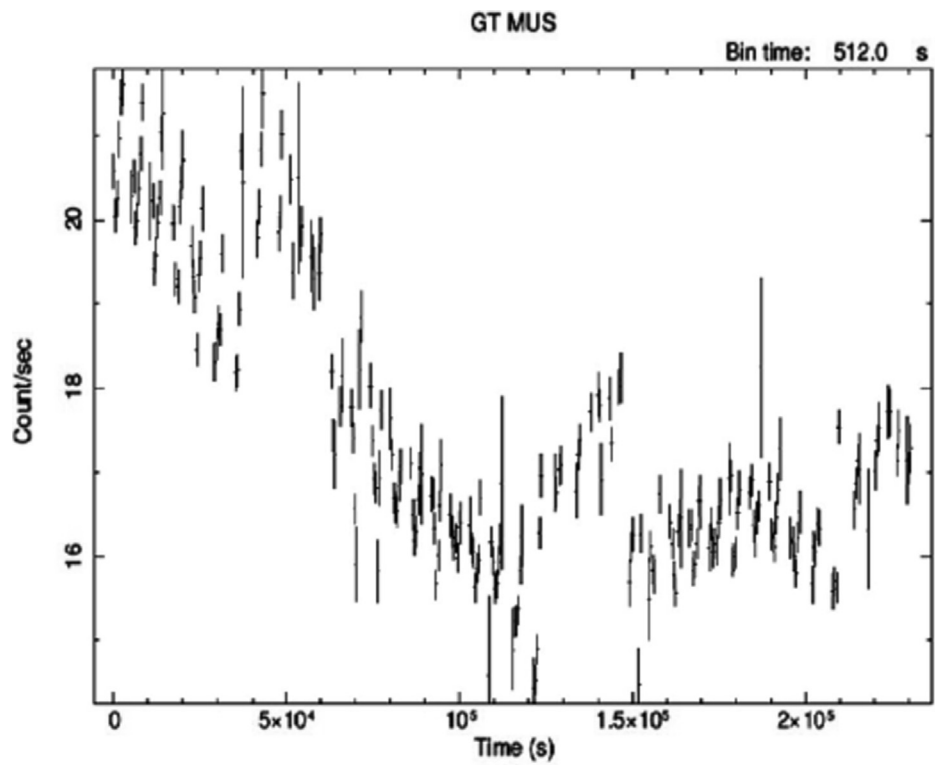
low background counting rate and a high energy range of about 0.2 – 600 keV. The XIS is a sensitive instrument in the energy range; 0.2 keV – 12 keV. XIS contains the back-illuminated (BI; XIS 1) and front-illuminated (FI; XIS 0 & 3) charge-coupled devices/sensors. A detailed description of the Suzaku satellite and its instrumentation can be found in research work (Mitsuda et al., 2007; Koyama et al., 2007a; Serlemitsos et al., 2007). Data reduction and analysis were done using version 2 of the standard Suzaku pipeline products; High Energy Astrophysical Software (HEASoft) version 6.90, XSPEC 12.8 version, and other HEASoft software packages installed in Ubuntu 18.04 operating system. We measure the flux of each source. The extraction of the Algol spectrum and background spectrum from a circular region of 200- and 140-arc-seconds radius respectively were done using XSELECT. During extraction, we ensured that the circular region covers 90% of the source's flux while the background events were extracted within the proximity of the source's flux. Moreover, proactive measures were also employed to exclude photon count/flux from apparent and/or nearby sources. This technique was repeated for GT Mus, but this time the extraction of the events was done from a circular region of 250- and 190- arc-second radius respectively. We subtracted the background spectrum from each source spectrum and the X-ray light curve of Algol and GT Mus were generated respectively (see Figs. 1 & 2). All the data generated from the light curve of each source were used. The Ancillary Response File and Response Matrix File (ARF & RMF) for the XIS sensors (XIS; 0, 1, 3) were built for each source data using Flexible Image Transport System Tools (FTOOLS), X-ray imaging spectrometer Ancillary response (xissamrf-gene) and X-ray imaging spectrometer response matrix file generator (xisrmf-gene; Ishisaki et al., 2007). XIS 0 & 3 sensors are the Suzaku-XRT front-illuminated chips and have similar features. Therefore, we merged their spectra and hereafter referred to them as XIS FI. However, XIS 1 is referred to as XIS BI since it is the back-illuminated chip. The XIS FI and XIS BI spectrum analysis for each source was done using XSPEC version 12.8.

We considered fitting the X-ray spectrum of each source in the 0.2 – 12 keV since Suzaku spectrometers are sensitive in these energy bands, and also to constrain the hydrogen column density and partial absorption covering fraction. The Algol's data was fitted in the 0.2 – 12 keV energy bands, and thereafter, modeled with absorption (tbabs) and thermal Bremsstrahlung models plus a Gaussian line with additional constant component [$const*tbabs*(bremss + gau)$] and hereby referred to as “*model 1*”. The model fitting parameters were allowed to be free. The hydrogen column density (N_{H}), and reduced Chi-squared obtained is $2.70 \times 10^{20} \text{ cm}^{-2}$; and 12.66 respectively. The emission line energy resolved was insignificant. The constant and line energy width parameters were frozen and the spectrum was re-fitted. The value of the reduced Chi-squared was unchanged and the value of the resolved line



Start Time 14167 15:44:58:564 Stop Time 14169 14:32:26:564

Fig. 1. Background subtracted Algol X-ray light curve.



Start Time 14446 12:30:28:184 Stop Time 14449 4:30:28:184

Fig. 2. Background subtracted GT Mus X-ray light curve.

energy is still insignificant. The line energy parameter was “steppar” in the interval of 6.6 keV to 6.8 keV, and the spectrum was re-fitted, but the value of the reduced Chi-squared and N_{H} remain unchanged with zero null hypothesis probability. Therefore, “*model 1*” did not give a good statistical fit. We were unable to resolve the 6.7 keV emission line using “*model 1*”. The Algol X-ray spectrum was re-normalized and the thermal Bremsstrahlung model was replaced with power-law model [*const*tbabs*(power-law + gau)*], and hereby referred to as “*model 2*”. Thereafter, the fitting procedure was repeated. The N_{H} , resolved line energy, and reduced Chi-squared obtained is $1.520 \times 10^{21} \text{ cm}^{-2}$, 6.61 keV, and 14.36 respectively. The value of the reduced Chi-squared is above the acceptable limit; < 2.0 , and this indicates that “*model 2*” also did not give a good statistical fit. Therefore, the model did not reproduce the data very well. Physical inspection of the obtained Algol’s X-ray spectrum shows that in the energy bands $< 2.0 \text{ keV}$ and $> 10.0 \text{ keV}$, the model did not fit the data very well. Moreover, fitting the X-ray spectrum down to the energy level below 2 keV and above 10 keV did not give a good statistical fit. Therefore, Algol’s X-ray spectrum below 2.0 keV and above 10.0 keV was ignored using XSPEC *ignore* command. Now, we repeated the aforementioned fitting procedure in the energy range 2 – 10 keV using “*model 1*” and “*model 2*” respectively. In each model, we were able to resolve line energy at 6.66 keV, though the value of the absorption column density obtained was very low. Moreover, the value of null hypothesis probability is not zero, but the value of the reduced Chi-squared (~ 2.3) is greater than the acceptable limit. We later employed the same technique in fitting and modeling GT Mus data in the 2.0 – 10.0 keV as we did with Algol using “*model 1*” and “*model 2*” respectively. In each model, we were able to resolve line energy at 6.68 keV. However, absorption column density and reduced Chi-squared value obtained using “*model 1*” is $5.42 \times 10^{13} \text{ cm}^{-2}$ and 1.97 respectively whereas that of “*model 2*” is $9.94 \times 10^{21} \text{ cm}^{-2}$ and 1.96 respectively. Here, the value of the reduced Chi-squared is below the acceptable limit but it is still high. We inspected the spectrum again and observed that the sources’ data and the models at 9.0–10.0 keV energy bands are not well aligned. This suggests that the signal to noise ratio is very low in these energy bands especially that of Algol. We reconsider fitting the Algol and GT Mus data in the 2.0 – 9.0 keV energy bands. We used XSPEC *ignore* command to ignore energy band above 9.0 keV band. We re-fitted the Algol data in the 2.0 – 9.0 keV energy bands and thereafter modeled the data with “*model 1*”. The emission line at 6.66 keV was resolved, but the value of the hydrogen column density (N_{H}), and Chi-squared is 1.4×10^{15} and 2.107 respectively. Some fitting parameters was frozen, “thawed” and “steppar” in order to obtain a good statistical fit, but the spectral fitting was not improved as much as expected. We repeated the same technique on Algol data using “*model 2*” and we were able to obtain the value of N_{H} and Chi-

squared value of 9.48×10^{21} and 1.9 respectively. We repeated the whole procedure by fitting the GT Mus data in the 2.0 – 9.0 keV using “*model 1*” and “*model 2*”. We froze, “thawed” and “steppar” some fitting parameters. In each model, thermal emission line at 6.68 keV was resolved, but the Chi-squared value obtained is above the acceptable limit. Therefore, “*model 1*” and “*model 2*” did not give a good-statistical fit of the Algol and GT Mus in the 2.0 – 9.0 keV energy bands. As a result, we include more models that can reproduce the data very well with a good statistical fit. This time, we replaced the absorption model (*tbabs*) with a partial covering fraction absorption model (*pcfabs*) in “*model 1*” and include an additional optically thin thermal plasma model (*apec*). That is, *const*pcfabs*(bremss + gau + apec)* and hereby referred as “*model 3*”. Starting with Algol, the X-ray spectrum/data was re-normalized. The spectral fitting was done in the 2.0 – 9.0 keV energy bands, and thereafter modeled with “*model 3*”. The fitting parameters were allowed to be free except element abundance and the redshift that was frozen. The line energy parameter was “steppar” and emission line energy at 6.66 keV was resolved with N_{H} , partial covering fraction, and reduced Chi-squared of $1.4 \times 10^{22} \text{ cm}^{-2}$, 0.95 and 1.74 respectively. We later froze the constant component, partial covering fraction, line energy width and some other parameters to see if we can obtain an improved good statistical fit, but the changes in the value of the reduced Chi-squared was not significant. Thence, all the frozen parameters were thawed, the X-ray spectrum was modeled and re-fitted. Later, the XSPEC *error* command was used to estimate the error in each parameter. An improved good Chi-statistical fit and degree of freedom was achieved with a reduced Chi-squared value of ~ 1.32 (see Table 1). Later, the Algol’s X-ray spectrum was re-normalized, and thereafter modeled with “*model 4*” [*const*pcfabs*(power-law + gau + apec)*]. The same fitting procedure as in “*model 3*” was implemented and we were able to resolve a 6.7 keV emission line with N_{H} and reduced Chi-squared of $4.75 \times 10^{22} \text{ cm}^{-2}$ and 1.29 respectively. The aforementioned fitting technique using “*model 3*” and “*model 4*” was employed in fitting the GT Mus data in the 2.0 – 9.0 keV energy bands, and a good-statistical fit were achieved (see Table 1). Table 1 shows the best-fit spectral parameters of Algol and GT Mus obtained using “*model 3*” and “*model 4*” only, and the results and discussion follow suit.

3. Results

Table 1 shows the best-fit spectral parameters of Algol and GT Mus in the 2.0 – 9.0 keV energy bands obtained with “*model 3*” and “*model 4*”. The spectral parameters errors with a 90% confidence limit (see Table 1) reported in this work are obtained from the XSPEC *error* command. Figs. 1 & 2 shows the background-subtracted X-ray light-curve of Algol and GT Mus respectively. Figs. 3 and 4 shows the X-ray spectrum of Algol and GT Mus when

Table 1
Spectral parameters of Algol and GT Mus in the 2 – 9 keV bands.

Spectral Parameters	Algol	GT Mus
$E_{6.7}^{(M3)}$	6.66 ± 0.03	6.67 ± 0.06
$EW_{6.7}^{(M3)}$	501_{-53}^{+47}	308_{-38}^{+16}
$F_{count}^{(M3)}$	$(0.533 \pm 0.003) \times 10^{-3}$	$(0.457 \pm 0.002) \times 10^{-3}$
$KT^{(M3)}$	4.64 ± 0.31	4.76 ± 0.14
$F_{6.7}^{(M3)}$	$(0.97 \pm 0.42) \times 10^{-4}$	$(1.078 \pm 0.22) \times 10^{-4}$
$\chi^2(M3)$	1394.81	2293.05
d.o.f. ^(M3)	1053	1480
$R\chi^2(M3)$	1.32	1.54
$N_H^{(M3)}$	$(2.53 \pm 0.34) \times 10^{22}$	$(5.50 \pm 0.75) \times 10^{22}$
$C^{(M3)}$	0.95 ± 0.07	0.81 ± 0.15
$KT_a^{(M3)}$	2.29 ± 0.03	2.39 ± 0.05
$PP_{index}^{(M4)}$	2.68 ± 0.026	2.73 ± 0.02
$F_{count}^{(M4)}$	$(9.95 \pm 0.08) \times 10^{-2}$	$(8.95 \pm 0.03) \times 10^{-2}$
$E_{6.7}^{(M4)}$	6.66 ± 0.04	6.70 ± 0.01
$F_{6.7}^{(M4)}$	$(0.973 \pm 0.05) \times 10^{-4}$	$(1.078 \pm 0.03) \times 10^{-4}$
$EW_{6.7}^{(M4)}$	522_{-19}^{+23}	329_{-34}^{+21}
$\chi^2(M4)$	1362.73	2242.68
d.o.f. ^(M4)	1056	1524
$R\chi^2(M4)$	1.29	1.47
$N_H^{(M4)}$	$(4.75 \pm 0.65) \times 10^{22}$	$(6.65 \pm 0.42) \times 10^{22}$
$C^{(M4)}$	0.55 ± 0.06	0.51 ± 0.03
$KT_a^{(M4)}$	2.23 ± 0.04	2.13 ± 0.02

KT = continuum temperature (keV), F_{count} = flux count (Photons⁻¹cm⁻²), $E_{6.7}$ = thermal Energy at 6.7 (keV), $EW_{6.7}$ = equivalent width of 6.7 keV emission line (eV), $(R\chi^2)$ = Reduced chi-squared, d.o.f. = degrees of freedom, PP_{index} = power law photon index, $F_{6.7}$ = flux of the 6.7 keV emission line (Photons s⁻¹cm⁻²). (B) and (P) is the Bremsstrahlung model and Power-law model spectral parameters respectively, N_H = hydrogen column density (cm⁻²), KT_a = plasma temperature (keV) of the apec model, C = partial absorption covering matter, χ^2 = Chi-squared statistics, (M3) and (M4) is the “model 3” and “model 4.”

modeled with “model 3” which is identical to respective spectrum of the Algol and GT Mus when modeled with “model 4” (not shown).

Thence, both “model 3” and “model 4” give a good statistical fit and reproduce the data of Algol and GT Mus very well in the 2.0 – 9.0 keV energy bands with best-fit spectral parameters shown in Table 1.

The peak of the XIS BI (red) and XIS FI (black) spectrum curve in Figs. 3 and 4 respectively on the energy axis corresponds to a 6.7 keV emission line.

Fig. 3 shows the X-ray spectrum of Algol fitted in the 2.0 – 9.0 keV energy bands. The fitted data are shown by crosses whereas the best-fit model (“Model 3”) is represented by solid and broken lines in the upper panel. The spectrum of the X-ray Imaging Spectrometer (XIS) Back-illuminated (BI) and Front-illuminated (FI) sensor or detector is represented by red and black color respectively. The two curves that emerged at flux count of 10⁻⁴ counts/s/keV and rise to the peak of respective XIS BI and XIS FI spectrum is the Gaussian line. The peak of the curve of XIS BI and XIS FI in the Algol X-ray spectrum corresponds to a strong emission line at 6.7 keV. The ratio of the fitted data to the best-fit model is shown in the lower panel. Moreover, the X-ray spectrum of Algol when fitted with the “Model 4” is identical to that obtained with the “Model 3”, but their spectral parameters are different (see Table 1).

Fig. 4 shows the X-ray spectrum of GT Mus fitted in the 2.0 – 9.0 keV energy bands. The fitted data are shown by crosses whereas the best-fit model (“Model 3”) is repre-

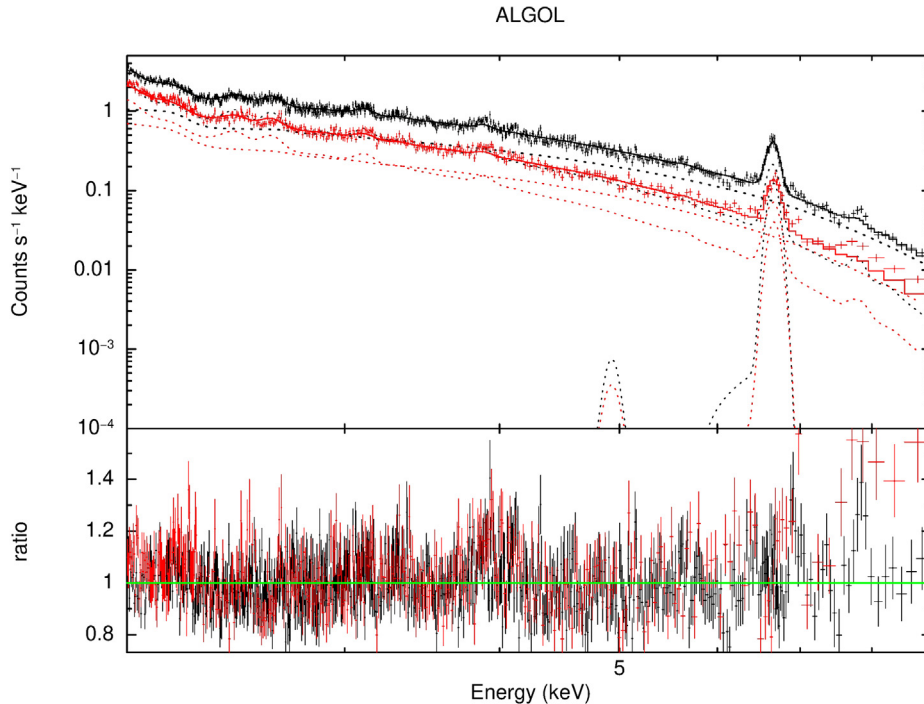


Fig. 3. Algol X-ray Spectrum in the 2.0 – 9.0 keV energy bands.

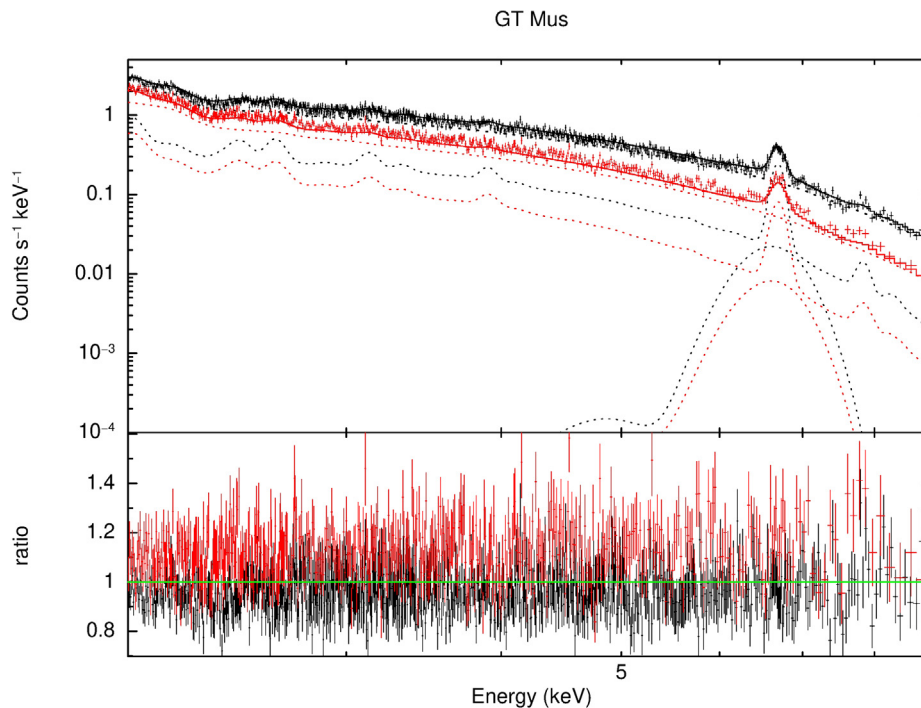


Fig. 4. GT Mus X-ray Spectrum in the 2.0 – 9.0 keV energy bands.

sented by solid and broken lines in the upper panel. The spectrum of the X-ray Imaging Spectrometer (XIS) Back-illuminated (BI) and Front-illuminated (FI) sensor or detector is represented by red and black color respectively. The two curves that emerged at flux count of 10^{-4} counts/s/keV and rise to the peak of respective XIS BI and XIS FI spectrum is the Gaussian line. The peak of the curve of XIS BI and XIS FI in the GT Mus X-ray spectrum corresponds to a strong emission line at 6.7 keV. The ratio of the fitted data to the best-fit model is shown in the lower panel. Moreover, the X-ray spectrum of Algol when fitted with the “*Model 4*” is identical to that obtained with the “*Model 3*”, but their spectral parameters are different (see Table 1).

4. Discussion

The X-ray light-curves (Figs. 1 and 2) show that each source has a typical signature of stellar flare and chromospheric activities on a time scale of hours to days. The X-ray light-curves show variations in brightness and aperiodic process; flickering behavior. The quiescent and flared phases of the light curves are due to starspot evolution and coronal/chromospheric activities. Both Algol and GT Mus exhibit long duration cyclic variations in brightness on timescale of hours to days though the signature of their stellar flare is different. Thus, Algol shows sporadic rapid rise and decay episodes with high amplitude whereas GT Mus shows a quasi-periodic episodes with low amplitude.

The sporadic flared epoch of Algol show a rapid rise and decay with high amplitude on timescales between 50 and 90 kiloseconds whereas the flared epoch of GT Mus show low

amplitude in quasi-periodic pattern. These are due to changes in the activity structure of the starspot. Flare activities in Algol started with “minute” changes in the brightness. By inspection, Algol’s light curve shows that there is a gradual increase in the flaring activities between 0 and 50 kilo-seconds. These time scales indicate the quiescent stages and little variation in brightness. Thereafter, a dramatic sudden increase in brightness was observed till the flaring activities reach their peak. These indicate fast rise in the stellar flares on time scales of 50 – 60 kiloseconds. Thereafter, a gradual decay ensues immediately as the chromospheric/flaring activities decrease, and this happens on time scales of 60 – 150 kiloseconds. This track of the light curve obeys the exponential decay law (Schmitt, Ness, & Franco, 2003; Eze A., et al., 2017; Sasaki et al., 2021). The gradual decay could be due to eclipsing of flaring plasma by the B-type star on timescales, though intrinsic variability and/or location of the active regions on the surface of the system in line of sight of observation could also contribute (Ottmann, 1994; Schmitt & Favata, 1999). During the time intervals of 50 – 90 kiloseconds, Algol exhibits intense sporadic and violent chromospheric activities; an indication of strong magnetic activities/ starspot evolution; hence the flaring epochs. At time scales above 150 kiloseconds, Algol embarked on another phase of cyclic-variation. On the other hand, the signature of stellar flare/chromospheric activities of GT Mus is different from that of Algol. GT Mus exhibit quasi-sinusoidal cyclic-variations on time scales of hours to days. The amplitude of variations in brightness is low during time intervals of 0 – 40 kiloseconds (0 – 11 h) and 60 – 110 kiloseconds

(0.69 – 1.27 days) respectively, and these phases obey the exponential decay law (Schmitt, Ness, & Franco, 2003; Sasaki et al., 2021). These epochs with quasi-periodic and low amplitude variations in brightness depict the quiescent stages of GT Mus. On time scales of 40 – 60 kilo-seconds (0.46 – 0.69 days) and 110 – 150 kilo-seconds (1.27 – 1.73 days), GT Mus exhibits intense flaring/ chromospheric activities; the flaring epochs. During the interval of 150 – 200 kilo-seconds (1.73 – 2.31 days), GT Mus flared again, but the amplitude of the flaring activities is not like the previous flaring epochs. There is a short periodic rise and fall in the variations of brightness of GT Mus.

The flickering behavior and signature of the flare activities in GT Mus during quiescent and flared epoch are not violent and sporadic when compared to that of Algol, but both sources exhibit intense dramatic changes; hence, star-spot evolution in each source differs. Therefore, the individual source has different signatures of stellar flare/ chromospheric activities as well as cyclic-variation in brightness on timescales of hours to days. This suggests that the magnitude of chromospheric/flaring activities during the quiescent stages of Algol and GT Mus differs. The coronal temperature and amplitude of variations in brightness during quiescent stages are low when compared to the temperature and brightness of their respective flaring epochs (Van den Oord, & Mewe, 1989; Singh et al., 1996; Nordon & Behar, 2007; Tsuboi et al., 2016). Both Algol's and GT Mus' light-curve shows long-duration stellar flare/ chromospheric activities, but the signature of the Algol's light curve is sporadic whereas that of GT Mus light-curve is quasi-periodic. The difference in the light-curve signature of the sources is a result of the flickering behavior of the churning particles/plasma in the coronae during star-spot evolution. The modeled spectra show that the plasma temperature (kT) in each source corona range between 3 keV and 4.8 keV (see Table 1) and this suggests that 6.7 keV photon-counts/fluxes dominate the coronae of the sources during the observation. This affirms the results of Warwick (2014) which inferred that the temperature of the plasma responsible for the generation of the 6.7 keV emission line lies in the range; $3 < kT < 5$ keV. The thermal emission line at 6.7 keV in the coronae is an indicator of chromospheric activities. Photo-ionization/collisional excitation of energetic particles during the quiescent and flared epochs of each source is responsible for the production of a thermal emission line at 6.7 keV. We resolved the hard energy spectrum at 6.7 keV and equivalent width (EW) in each source's stellar flare data in the 2.0 – 9.0 keV bands. In the upper panel of each source spectrum, (Figs. 3 and 4), the fitted data and best-fit model are shown by crosses and solid and broken lines respectively. The red and black spectrum in the upper panel in Figs. 3 and 4 represents the XIS BI and XIS FI respectively. The peak of the curve of XIS BI and XIS FI in each source's spectrum corresponds to a strong emission line at 6.7 keV (see Figs. 3 and 4). The lower panel of each Figure portrays the ratio of the fitted data to the best-fit model. The “model 3” and “model 4”

gave good statistical fit with acceptable spectral fit parameters (see Table 1). The resolved emission line at 6.7 keV is similar to the results of previous spectroscopic analyses done on the stellar flares of Algol and GT Mus (Stern et al., 1992; Antunes et al., 1994; Favata & Schmitt, 1999; Yang et al., 2011; Eze et al., 2015b; Eze, et al., 2017, 2019; Goodwill et al., 2019).

The light curve, X-ray spectrum, and 6.7 keV emission line resolved in this work are more robust when compared to that of the other satellite observations (ASCA, BeppoSAX, ROSAT, XMM-Newton, etc.). This could be either the proportional counter and/or charge-coupled-device (CCD) cameras of the X-ray telescopes of these satellites are contaminated by nearby sources/Perseus clusters or they don't have sufficient sensitivity. For instance, ROSAT has limited spectral coverage and limited resolution (Antunes et al., 1994; Ottmann & Schmitt, 1996) whereas Suzaku have high spectral coverage in the 0.2 – 12 keV X-ray energy bands. Moreover, the measure at which photon counts/flux extraction and data reduction are done can also affect the X-ray spectrum. The emission line at 6.7 keV obtained in each source also has a marked spectral similarity to the hard energy spectra of 6.7 keV observed in different Galactic ridge positions (Ebisawa et al., 2008; Yamauchi et al., 2009; Yuasa et al., 2012). The EW of the 6.7 keV emission line obtained in each source compared favorably with the EW (260 – 980 eV) of the 6.7 keV emission line depending on the Galactic ridge regions (Ebisawa et al., 2008; Yamauchi et al., 2009; Uchiyama et al., 2013; Warwick, 2014). Given this, CABs are coronally active stars and binaries, and they could account for numerous fast transient sources that emit strong thermal emission line at 6.7 keV during their quiescent and flared epochs in the Galactic ridge.

4.1. On the contribution of the 6.7 keV emission line from the stellar flares of CABs to the 6.7 keV X-ray emission line from the Galactic ridge

The 6.7 keV emission line is an elongated, strong X-ray K-shell line from He-like iron. It is seen as thin thermal hot plasma in all the observed regions of the Galactic ridge and/or plane (Ebisawa et al., 2008; Yamauchi et al., 2009; Revnivtsev et al., 2009). The Fe XXV $K\alpha$ (6.7 keV), emission line has been resolved from the stellar flare data of point sources observed by different X-ray detectors and/or satellites (GINGA, ASCA, ROSAT, Chandra, XMM-Newton, Suzaku, etc; Stern et al., 1992; Ottmann & Schmitt, 1996; Ebisawa et al., 2008; Yamauchi et al., 2009; Uchiyama et al., 2013). The spectrum of the 6.7 keV emission line from this work is similar to the hard energy spectrum of point sources believed to contribute significant fractions of the total luminosity of the 6.7 keV X-ray emission line in the Galactic ridge (Ebisawa et al., 2001, 2005, 2008; Yamauchi et al., 2009; Revnivtsev et al., 2009; Morihana et al., 2013). The equivalent width (EW) of the 6.7 keV emission line from the

Algol and GT Mus compares favorably with the EW (260 eV – 980 eV) of hard energy spectra of 6.7 keV emission line resolved from numerous Galactic point sources observed at different positions (Yamauchi et al., 2009; Yuasa et al., 2012; Uchiyama et al., 2013; Warwick, 2014; Eze, R. et al., 2015b). These stellar population sources exhibit a strong hard energy spectrum at 6.7 keV. The contribution of Galactic point sources to the total luminosity of GRXE is yet unresolved. In the X-ray energy band, (2 – 10 keV), several population sources account for different fractions of the total luminosity of GRXE. The probable candidate sources of GRXE are magnetic cataclysmic variables, active binaries, hard X-ray emitting Symbiotic Stars, X-ray active stars, coronally-active stars, and binaries (ABs; Revnivtsev et al., 2009; Yamauchi et al., 2009; Yuasa et al., 2010, 2012; Eze, R., 2014, 2015; Xu et al., 2016). These sources emit a 6.7 keV emission line during their quiescent and flared phases. Integrated hard energy spectra from these sources have accounted for the bulk of GRXE in the 6 – 7 keV energy range (Ebisawa et al., 2001, 2005, 2008; Revnivtsev et al., 2009; Yamauchi et al., 2009; Yuasa et al., 2010, 2012). The X-ray active stars and binaries are thermal source populations with broad X-ray fluxes. Their contributions to Fe K α -emission line at 6.7 keV during flared and quiescent epochs in the ratio of 2:1 have been inferred (Moriwana et al., 2013). Galactic source populations [dwarf stars, coronally active stars and binaries (ABs) and cataclysmic variables (CVs)], with intrinsic X-ray luminosity; 10^{28-34} ergs $^{-1}$ have accounted for a substantial fraction of $\sim 80 - 90$ % of GRXE (Ebisawa et al., 2005, 2008; Revnivtsev et al., 2009; Yamauchi et al., 2009). Warwick, (2014) estimated the contributions of the group of sources [coronally active stars and binaries (ASBs) and Cataclysmic variables (CVs)] in the 2 – 10 keV, and 6 – 10 keV energy bands and inferred that each group of sources accounted for 78% & 16%, and 62% & 21% of GRXE respectively. The coronal plasma temperature characterizing coronally active stars and binaries and cataclysmic variables thermal mix spectra ranges; 3 keV to 7 keV, and estimated EW ratio of 6.7 keV to 7.0 keV emission line is 3:1 (Warwick, 2014). This suggests that the photon counts/fluxes of the 6.7 keV emission line in the corona outstrip that of the 7.0 keV, and this could be the reason why the 6.7 keV emission line is seen in all the regions of the Galactic ridge (Yamauchi et al., 2009). Eze, R. et al. (2015b) also reported that X-ray stars and binaries during their quiescent and flared epochs contribute $\sim 70\%$ of 6.7 keV GRXE. These Galactic point sources have large spatial population density and their emission lines at 6.7 keV are indicators of strong intense stellar flares and chromospheric activities (Morris & Mutel, 1988; Gioia et al., 1990; Favata et al., 1995; Berdyugina, 2005; Warwick, 2014; Yoldas & Dal, 2017). The emission line at 6.7 keV resolved in this present work is remarkably similar to the 6.7 keV emission line of different point sources observed in the Galactic plane/ridge (Ebisawa et al., 2005, 2008; Revnivtsev et al., 2006a, b,

2009; Yamauchi et al., 2009; Yuasa et al., 2010, 2012). The EW of the 6.7 keV emission line resolved in the present work compares favorably with the EW of the 6.7 keV emission line from Galactic point sources (Ebisawa et al., 2008; Yamauchi et al., 2009; Warwick, 2014; Eze, R., et al., 2015b). Previous studies revealed that these Galactic point sources are the major contributors of GRXE (e.g. Ebisawa et al., 2005, 2008; Yamauchi et al., 2009; Revnivtsev et al., 2009; Yuasa et al., 2010; Matsuoka et al., 2011; Moriwana et al., 2013; Eze, R., et al., 2015b; Xu et al., 2016). These major contributors emitting strong thermal emission line at 6.7 keV have been classified as X-ray coronally-active dwarf stars and binaries of spectral F to M in H-R diagram (Vaiana et al., 1981; Strassmeier et al., 1988, 1993; Dempsey et al., 1993; Barrado et al., 1994, 1997, 1998; Montes et al., 1998; Gudel, 2004; Berdyugina et al., 2005; Sazonov et al., 2006; Demircan et al., 2006; Eker et al., 2008; Warwick, 2014; Pye et al., 2015; Xu et al., 2016; Tsuboi et al., 2016; Yoldas & Dal, 2017). Given this, CABs could account for a large number of fast transient sources that emit a 6.7 keV thermal emission line in the Galactic ridge and could be probable candidates of GRXE.

5. Conclusion

We have re-analyzed the stellar flare data of Algol and GT Mus. Starspot evolution, coronal/chromospheric activities in these sources explain the stellar flare formation and cyclic- variations in brightness. X-ray emission originates from the coronae of the magnetically active late-type evolved star of the binary system though in some CABs both component stars contribute significantly. Intense dramatic variations in brightness, emission of ions, and X-ray emission are characteristics of stellar flare/chromospheric/magnetic activities. Each source exhibits a typical signature of flaring/chromospheric activities on timescales of hours to days. We resolved the 6.7 keV emission line in each source's stellar flare data. The thermal emission line at 6.7 keV resolved in this work is remarkably similar to the 6.7 keV emission line of X-ray point sources observed from different Galactic ridge regions. The EW of 6.7 keV emission line of Algol and GT Mus compared favorably with previous studies.

CABs are coronally-active dwarf stars and binaries, with strong chromosphere/corona and intense stellar flare/chromospheric activities and X-ray emission. CABs are F to M spectral classes with large population density in 25 – 200 parsec of the Galactic plane. Algol and GT Mus are transient/variable flare star candidates of CABs, and they are X-ray emitters. Cumulative X-ray emission lines from numerous point sources observed in the Galactic ridge/plane give clues on the GRXE mechanism. We are of the view that CABs could account for a large number of Galactic fast-transients that emit thermal emission line at 6.7 keV, and could be probable candidates source of GRXE. Moreover, we suggest that the collection of similar CABs candidates along with CVs and other flare stars

could account for the total luminosity of the thermal emission line at 6.7 keV from the Galactic ridge.

Declaration of Competing Interest

The authors declare that they have no known competing financial interests or personal relationships that could have appeared to influence the work reported in this paper.

Acknowledgment

We are grateful to the Suzaku team for providing data and relevant files used in the analysis presented here. This research made use of data obtained from Data Archives and Transmission System (DARTS), provided by the Center for Science-satellite Operation and Data Archives (C-SODA) at the Institute of Space and Astronautical Science/ Japan Aerospace Exploration Agency (ISAS/JAXA). We are also grateful to Prof., R.N.C. Eze of the Department of Physics and Astronomy, University of Nigeria, Nsukka for his immeasurable assistance and guidance. Also, we thank the anonymous reviewers for their wonderful suggestions.

References

- Antunes, A., Nagase, F., White, N.E., 1994. ASCA observations of the coronal X-ray emission of Algol. *Astrophys J* 436, 83–86. <https://doi.org/10.1086/187638>.
- Audard, M., Gudel, M., Sres, A., Raassen, A.J.J., Mewe, R., 2003. A study of coronal abundances in RS CVn binaries*. *Astronomy & Astrophysics* 398, 1137–1149. <https://doi.org/10.1051/0004-6361:20021737>.
- Baron, F., Monnier, J.D., Pedretti, E., Zhao, M., Schaefer, G., Parks, R., Che, X., Thureau, N., Brummelaar, T.A., McAlister, H.A., Ridgway, S.T., Farrington, C., Sturmann, J., Sturmann, L., Turner, N., 2012. Imaging the Algol Triple system in the H Band with the Chara Interferometer. *Astrophys J* 752, 20. <https://doi.org/10.1088/0004-637X/752/1/20>.
- Barrado, D.Y.N., De Castro, E., Fernandez-Figueroa, M.J., Cornide, M., Lopez, R.J.G., 1998. The age-mass relation for chromospherically active binaries III. Lithium depletion in giant components*. *A & A* 337, 739–753.
- Barrado, D.Y.N., Fernandez-Figueroa, M.J., Lopez, R.J.G., De Castro, E., Cornide, M., 1997. The age-mass relation for chromospherically active binaries II. Lithium depletion in dwarf components***. *A & A arXiv:Astro-ph/9703199v1*.
- Barrado, D., Fernandez-Figueroa, M.J., Montesino, B., De Castro, E., 1994. The age-mass relation for chromospherically active binaries I. The evolutionary status. *Astronomy & Astrophysics* 290, 137–147.
- Berdyugina, S.V., 2005. Starspots: A key to the stellar dynamo. *Living Review Solar Physics* 2, 8. <https://doi.org/10.12942/lrsp-2005-8>.
- Benz, A.O., Guedel, M., 1994. X-ray/microwave ratio of flares and coronae. *A & A* 285, 621–630.
- Biazzo, K., Frasca, A., Henry, G.W., Catalano, S., Marilli, E., 2007. Photospheric and Chromospheric active regions in four Young Solar-Type stars. *Astrophys J* 656.
- Bleach, J.N., Wood, J.H., Smalley, B., Catalan, M.S., 2002. Echelle observations of chromospheric activity in post-common-envelope binaries. *Monthly Notice of the Royal Astronomical Society* 335, 593–609.
- Cao, D., Gu, S., 2015. Chromospheric activity and rotational modulation of the RS Canum Venaticorum binary V711 Tauri during 1998–2004. *MNRAS* 449, 1380–1390.
- Chung, S.M., Drake, J.J., Kashayap, V.L., Lin, L.W., Ratzlaff, P.W., 2004. Doppler Shifts and broadening and the structure of the X-ray emission from Algol. *Astrophys J* 606, 1184.
- Clarke, R.W., Davenport, J.R.A., Covey, K.R., Baranec, C., 2018. Flare Activity of Wide Binary Stars with Kepler. *Astrophys J* 853, 59.
- Collier, C.A., 1987. UBVR(I)c Photometry for Ca II Emission Stars Observations at MT John University Observatory and at MT Stromlo. *South African Astronomy Observatory Circ.* 11, 57–71.
- Covino, S., Panzera, M.R., Tagliaferri, G., Pallavicini, R., 2001. Quiescent and flare analysis for the chromospherically active star Gl 355 (LQHy). *The Astronomy & Astrophysics* 371, 973.
- Csizmadia, S.Z., Borkovits, T., Paragi, Z., Abraham, P., Szabados, L., Mosoni, L., Sturmann, L., Sturmann, J., Farrington, C., McAlister, H. A., ten Brummelaar, T.A., Turner, N.H., Klagyivik, P., 2009. Interferometric Observations of the Hierarchical Triple system Algol. *Astrophys J* 705, 436–445.
- Demircan, O., Eker, Z., Karatas, Y., Bilir, S., 2006. Mass loss and orbital period decrease in detached chromospherically active binaries. *Monthly Notice of the Royal Astronomical Society* 366, 1511–1519. <https://doi.org/10.1111/j.1365-2966.2005.09948.x>.
- Dempsey, R.C., Linsky, J.L., Fleming, T.A., Schmitt, J.H.M.M., 1993. The ROSAT all-sky survey of active binary coronae. I. quiescent fluxes for the RS Canum Venaticorum systems. *The Astrophysical Journal Supplement Series* 86, 599–609.
- Drake, J.J., 2003. Chemical fractionation and abundances in coronal plasma. *Adv. Space Res.* 32, 945–954. [https://doi.org/10.1016/S0273-1177\(03\)00296-5](https://doi.org/10.1016/S0273-1177(03)00296-5).
- Drake, J.J., Peres, G., Orlando, S., Laming, J.M., Maggio, A., 2000. On stellar coronae and solar active regions. *Astrophys. J.* 545, 1074–1083. <https://doi.org/10.1086/317820>.
- Drake, J.J., Laming, J.M., Widing, K.G., 1997. Stellar coronal abundances. V. Evidence for the first ionization potential effect in alpha Centauri. *The Astrophysical Journal* 478, 403. <https://doi.org/10.1086/303755>.
- Ebisawa, K., Yamauchi, S., Tanaka, Y., Koyama, K., Ezoe, Y., Bamba, A., Kokubun, M., Hyodo, Y., Tsujimoto, M., Takashi, H., 2008. Spectral study of Galactic ridge X-ray emission with Suzaku. *Publication of the Astronomical Society of Japan* 60, 223–229.
- Ebisawa, K., Tsujimoto, M., Paizis, A., Hamaguchi, K., Bamba, A., Cutri, R., Kaneda, H., Maeda, Y., Sato, G., Senda, A., Ueno, M., Yamauchi, S., Beckmann, V., Courvoisier, T.J.L., Dubath, P., Nishihara, E., 2005. Chandra Deep X-Ray observation of A Typical Galactic Plane Region and Near-Infrared Identification. *Astrophys J* 635, 214–242.
- Ebisawa, K., Maeda, Y., Kaneda, H., Yamauchi, S., 2001. Origin of the Hard X-ray Emission from the Galactic Plane. *Science* 293 (5535), 1633–1635. <https://doi.org/10.1126/science.1063529>.
- Eker, Z., Filiz Ak N., Bilir, S., Dogru, D., Tüysüz, M., Soyduğan, E., Bakis, H., B. Ugras, B., Soyduğan, F., Erdem, A., & Demircan, O., 2008. A catalog of chromospherically active binary stars (third edition). *Monthly Notice of the Royal Astronomy Society* 389, 1722–1726. [Doi:10.1111/j.1365-2966.2008.13670.x](https://doi.org/10.1111/j.1365-2966.2008.13670.x).
- Eze, R.N.C., Ebisawa, K., Eze, A., Nwafiah, J., Esaenwi, S., Okeke, P.N., Smith, R., 2015b. The 6.7 keV Emission line from Stars and the Galactic Ridge X-ray Emission. *MNRAS* 000.
- Eze, A.C., Esaenwi, S., Chima, A.I., 2019. The 6.7 keV Line Emission from the Stellar Flare of Algol. *Journal of High Energy Physics, Gravitation and Cosmology* 5, 1090–1097.
- Eze, A.C., Eze, R.N., Esaenwi, S., 2017. On the Contribution of the 6.7 keV Line Emission of the Algol Binary System to the 6.7 keV Line Emission from the Galactic Ridge. *Turkish Journal of Physics* 41, 277–284.
- Favata, F., Micela, G., Reale, F., Sciortino, S., Schmitt, J.H.M.M., 2000. The structure of Algol's corona: a consistent scenario for the X-ray and radio emission. *A & A* 362, 628–634.
- Favata, F., Schmitt, J.H.M.M., 1999. Spectroscopic analysis of a super-hot giant flare observed on Algol by BeppoSAX on 30 August 1997. *A & A* 350, 900–916.

- Favata, F., Micela, G., Sciortino, S., 1995. The space density of active binaries from X-ray surveys. *A & A* 298, 482–488.
- Galvez, M.C., Montes, D., Fernandez-Figueroa, M.J., De Castro, E., Cornide, M., 2009. Multiwavelength Optical Observations of two Chromospherically active binary systems: V789 MON and GZ LEO*. *The Astronomical Journal* 137, 3965–3975. <https://doi.org/10.1088/0004-6256/137/4/3965>.
- Garcia, M., Baliunas, S.L., Conroy, M., Johnston, M.D., Ralph, E., Roberts, W., Schwartz, D.A., Tonry, J., 1980. Optical Identification of H0123+075 AND 4U 1137–65: Hard X-ray emission from RS Canum Venaticorum systems. *Astrophys J* 240, L107–L110.
- Garcia-Alvarez, D., Drake, J.J., Testa, P., 2009. Neon and chemical fractionation trends in late-type stellar atmospheres. *AIP Conf. Proc.* 1094, 796–799. <https://doi.org/10.1063/1.3099236>.
- Gioia, I.M., Maccacaro, T., Schild, R.E., Wolter, A., Stocke, J.T., Morris, S.L., Henry, J.P., 1990. The Einstein Observatory extended medium-sensitivity survey. I. X-ray data and analysis. *The Astrophysical Journal Supplement Series* 72, 567–619.
- Goodwill, C.O., Esaenwi, S., Eze, A.C., 2019. Contribution of GT-Mus to the 6.7 keV Emission Line from the Galactic Ridge. *International. J. High Energy Phys.* 6 (1), 13–16. <https://doi.org/10.11648/j.ijhep.20190601.12>.
- Gudel, M., 2004. X-ray astronomy of stellar coronae. *Astron. Astrophys. Rev.* 12, 71–237. <https://doi.org/10.1007/s00159-004-0023-2>.
- Hall, D.S., 1976. Multiple Periodic Variable Stars. In *International Astronomical Union Colloquium* 29, 287.
- Harnden, F., Fabricant, D., Topka, K., Flannery, B., Tucker, W., Gorenstein, P., 1977. A soft X-ray image of the Algol region. *Astrophys J* 214, 418–422.
- Hearnshaw, J.B., Komonjinda, S., Skuljan, J., Kilmartin, P.M., 2012. A study of non-Keplerian velocities in observations of spectroscopic binary stars. *MNRAS* 427, 298–310.
- Ishisaki, Y., Maeda, Y., Fujimoto, R., Ozaki, M., Ebisawa, K., Takahashi, T., Ueda, Y., Ogasaka, Y., Ptak, A., Mukai, K., Hamaguchi, K., Hirayama, M., Kotani, T., Kubo, H., Shibata, R., Ebara, M., Furuzawa, A., Izuka, R., Inoue, H., Mori, H., Okada, S., Yokoyama, Y., Matsumoto, H., Nakajima, H., Yamaguchi, H., Anabuki, N., Tawa, N., Nagai, M., Katsuda, S., Hayashida, K., Bamba, A., Miller, E.D., Sato, K., Yamasaki, N.Y., 2007. Monte Carlo Simulator and Ancillary Response Generator of Suzaku XRT/XIS System for Spatially Extended Source Analysis. *Publication Astronomical Society of Japan* 59, S113–S132.
- Jones, K.L., Stewart, R.T., Nelson, G.J., 1995. The radio corona of HD 101379. *Monthly Notice of the Royal Astronomy Society* 274, 711–716.
- Koyama, K., Tsunemi, H., Dotani, T., Bautz, M., Hayashida, K., Tsuru, T., Matsumoto, H., Ogawara, Y., Ricker, G., Doty, J., Kissel, S., Foster, R., Nakajima, H., Yamauchi, H., Mori, H., Sakano, M., Hamaguchi, K., Nishiuchi, M., Miyata, E., Torii, K., Namiki, M., Katsuda, S., Matsuura, D., Miyauchi, T., Anabuki, N., Tawa, N., Ozaki, M., Murakami, H., Maeda, Y., Ichikawa, Y., Prigozhin, G., Boughan, E., Lamarra, B., Miller, E., Burke, B., Gregory, J., Pillsbury, A., Bamba, A., Hiraga, J., Senda, A., Katayama, H., Katayama, H., Tsujimoto, M., Kohmura, T., Tsuboi, Y., Awaki, H., 2007. X-ray Imaging Spectrometer (XIS) on Board Suzaku. *Publication of the Astronomical Society of Japan* 59, 23–33.
- Koyama, K., Makishima, K., Tanaka, Y., 1986. Thermal X-ray Emission with intense 6.7 keV iron line from the Galactic ridge. *Publication of the Astronomical Society of Japan* 38, 121–131.
- Krivonos, R., Revnivtsev, M., Churazov, E., Sazonov, S., Grebenev, S., Sunyaev, R., 2007. Hard X-ray emission from the Galactic ridge*. *The Astronomy & Astrophysics* 463, 957–967. <https://doi.org/10.1051/0004-6361:20065626>.
- Lestrade, J.F., Phillips, R.B., Hodges, M.W., Preston, R.A., 1993. VLBI Astrometric Identification of the Radio Emitting region and determination of the orientation of the close binary. *Astrophys J* 410, 808–814.
- Matsuoka, M., Sugizaku, M., Tsuboi, Y., Yamazaki, K., Matsumura, T., Mihara, T., Serino, M., Nakahira, S., Yamamoto, T., Ueno, S., Negoro, 2011. A contribution of Stellar flares to the GRXE–based on MAXI Observation. *NARIT Conference Series* 1, 246–249.
- Mitsuda, K., Bautz, M., Inoue, H., Kelley, R., Koyama, K., Kunied, H., Makishima, K., Ogarawa, Y., Petre, P., Takaha, T., et al., 2007. The X-Ray Observatory Suzaku. *Publication of the Astronomical Society of Japan* 59, 1–7.
- Montes, D., Lopez-Santiago, J., Fernandez-Figueroa, M.J., Galvez, M.C., 2001. Chromospheric activity, lithium and radial velocities of single late-type stars possible members of young moving groups ***. *Astronomy & Astrophysics* 379, 976.
- Montes, D., Fernandez-Figueroa, M.J., De Castro, E., Cornide, M., Latorre, A., Sanz-Forcada, J., 2000. Multiwavelength optical observations of Chromospherically active binary systems III. High-resolution echelle spectra from Ca II H & K to Ca II IRT*. *A & A* 146, 103.
- Montes, D., Ramsey, L.W., Welty, A.D., 1999. Library of medium-resolution fiber Optic echelle spectra of F, G, K, and M field dwarf to giant stars. *The Astrophysical Journal Supplement Series* 123, 283–293.
- Montes, D., Sanz-Forcada, J., Fernandez-Figueroa, M.J., De Castro, E., Poncet, A., 1998. Multiwavelength optical observations of Chromospherically active binary systems II. EZ Pegasi*. *A & A* 330, 155–168.
- Montes, D., Ramsey, L.W., 1999. A long-duration flare in the X-ray/EUV selected Chromospherically active binary 2RE J0743+224. *ASP Conference Series*.
- Montes, D., Fernandez-Figueroa, M.J., Cornide, M., De Castro, E., 1996. The behavior of the excess Ca II H & K H α emission in the chromospherically active binaries*. *The. A & A arXiv:Astro-ph/9511125*.
- Morel, T., Micela, G., Favata, F., Katz, D., Pillitteri, I., 2003. The photospheric abundances of active binaries II. Atmospheric parameters and abundance patterns for 6 single-lined RS CVn systems**,*. *Astronomy&Astrophysics* 412, 495–512. <https://doi.org/10.1051/0004-6361:20031469>.
- Morihana, K., Tsujimoto, M., Yoshida, T., Ebisawa, K., 2013. X-ray Point Source Populations constituting the Galactic ridge X-ray Emission. *Astrophys J* 766, 14.
- Morris, D.H., Mutel, R.L., 1988. Radio Emission from RS CVn Binaries III. A VLA Survey of 103 Systems. *The Astronomical Journal* 95 (1).
- Murdoch, K.A., Hearnshaw, J.B., Kilmartin, R.M., Gilmore, A.C., 1995. A photometric and orbital analysis of GT Muscae. *Monthly Notice of the Royal Astronomy Society* 276, 836–846.
- Nordon, R., Behar, E., 2007. Six large coronal X-ray flares observed with Chandra. *A & A* 464, 309–321.
- O’Neal, D., 2006. On the use of line Depth ratios to measure starspot properties on magnetically active stars. *Astrophys J* 645, 659–663.
- O’Neal, D., Saar, S.H., Neff, J.E., 1998a. Spectroscopic Evidence for non uniform starspot properties on II Pegasi. *Astrophys J* 501, L73–L76.
- O’Neal, D., Neff, J.E., Saar, S.H., 1998b. Measurements of starspot parameters on active stars using molecular bands in Echelle spectra. *Astrophys J* 507, 919–937.
- Ottmann, R., Schmitt, J.H.M.M., 1996. ROSAT Observation of a giant X-ray flare on Algol: evidence of abundance variation? *A & A* 307, 813–823.
- Ottmann, R., 1994. Structure and stability of the X-ray coronal of Algol. *A & A* 286, L27–L30.
- Pallavicini, R., Randich, S., Giampapa, M.S., 1992. Lithium in RS CVn binaries and related chromospherically active stars* I. Observational results. *Astronomy & Astrophysics* 253, 185–198.
- Pallavicini, R., Golub, L., Rosner, R., Vaiana, G.S., Ayres, T., Linsky, J. L., 1981. Relations among Stellar X-Ray Emission Observed from Einstein, Stellar Rotation and Bolometric Luminosity. *Astrophys. J.* 248, 279–290.
- Peterson, W.M., Mutel, R.L., Lestrade, J.-F., Gudel, M., Goss, W.M., 2011. Radio Astrometry of the Triple systems Algol and UX ARIETIS. *Astrophys J* 737, 104. <https://doi.org/10.1088/0004-637X/737/2/104>.

- Pettersen, B.R., 1989. A review of stellar flares and their characteristics. *Sol. Phys.* 121, 299–312. https://doi.org/10.1007/978-94-009-1017-1_20.
- Pye, J.P., Rosen, S., Fyfe, D., Schröder, A.C., 2015. A survey of stellar X-ray flares from the XMM-Newton serendipitous source catalog: Hipparcos-Tycho cool stars*, **, ***. *A & A* 581, A28. <https://doi.org/10.1051/0004-6361/201526217>.
- Revnivtsev, M., Sazonov, S., Churazov, E., Forman, W., Vikhlinin, A., Sunyaev, R., 2009. Discrete sources as the Origin of the Galactic X-ray ridge emission. *Nature* 458, 1142–1144.
- Revnivtsev, M., Sazonov, S., Gilfanov, M., Churazov, E., Sunyaev, R., 2006a. Origin of the Galactic ridge X-ray emission. *A & A* 452, 169–178.
- Revnivtsev, M., Molokov, S., Sazonov, S., 2006b. Map of the Galaxy in the 6.7 keV emission line. *Monthly Notice of Royal Astronomical Society* 373, L11–L15.
- Richards, M.T., 1993. Circumstellar material in Algol: A study of the Balmer line profiles. *The Astrophysical Journal Supplementary Series* 86, 255–291.
- Sanz-Forcada, J., Favata, F., Micela, G., 2007. Eclipsed X-ray flares in binary stars: geometrical constraints on the flare's location and size*. *A & A* 466, 309–316.
- Sasaki, R., Tsuboi, Y., Iwakiri, W., Nakahira, S., Maeda, Y., Gendreau, K., Corcoran, M.F., Hamaguchi, K., Arzoumanian, Z., Markwardt, C.B., et al., 2021. The RS CVn type star GT Mus shows most energetic X-ray flares throughout the 2010s. *Astrophys J* 910, 25.
- Sazonov, S., Revnivtsev, M., Gilfanov, M., Churazov, E., Sunyaev, R., 2006. X-ray luminosity function of faint point sources in the Milky Way. *A & A* 450, 117–128. <https://doi.org/10.1051/0004-6361:20054297>.
- Schmitt, J.H.M.M., Ness, J.U., Franco, G., 2003. A Spatially Resolved Limb Flare on Algol B Observed with XMM-Newton. *A & A* 412, 849–855.
- Schmitt, J.H.M.M., Favata, F., 1999. Continuous heating of a giant X-ray flare on Algol. *Nature* 401, 44.
- Schnopper, H., Delvaile, J.P., Epstein, A., Helmken, H., Murray, S., 1976. Detection of X-rays from Algol (β Persei). *Astrophys J* 210, 75–77.
- Serlemitsos, P., Soong, Y., Chan, K., Okajima, T., Lehan, J., Maeda, Y., Itoh, K., Mori, H., Izuka, R., Itoh, A., Inoue, H., Okada, S., Yokoyama, Y., Itoh, Y., Ebara, M., Nakamura, R., Suzuki, K., et al., 2007. The X-Ray Telescope on board Suzaku. *Publication of the Astronomical Society of Japan* 59, 9–21.
- Singh, K.P., Drake, S.A., White, N.E., 1996. RS CVn versus Algol-type binaries: A comparative study of their X-ray emission. *Astrophys J* 111, 6.
- Singh, K.P., Drake, S.A., White, N.E., 1995. A study of X-ray emission from short-period Algol binaries. *Astrophys J* 445, 840–854.
- Söderhjelm, S., 1980. Geometry, and Dynamics of the Algol System. *Astronomy & Astrophysics* 89, 100–112.
- Stern, R., Uchida, Y., Tsuneta, S., Nagase, F., 1992. GINGA Observation of X-ray Flares on Algol. *Astrophys J* 400, 321–329.
- Strassmeier K. G., Hall D. S., Fekel F. C., & Scheck M., 1993. A catalog of Chromospherically active binary stars (Second Edition). *Astronomy & Astrophysics Supplement Series*, 100, 173-225.
- Strassmeier, K.G., Hall, D.S., Zeilik, M., Nelson, E., Eker, Z., Fekel, F. C., 1988. A catalog of Chromospherically active binary stars. *Astron. Astrophys., Suppl. Ser.* 72, 291–345.
- Testa, P., Saar, S.H., Drake, J.J., 2015. Stellar activity and coronal heating: An overview of recent results. *Philosophical Transactions of Royal Society A* 373, 20140259.
- Testa, P., 2010. Element abundances in X-ray emitting plasma in stars. *Space Science Review* 157, 37–55. <https://doi.org/10.1007/s11214-010-9714-3>.
- Tsuboi, Y., Sasaki, R., Sugawara, Y., Matsuoka, M., 2017. A universal correlation between the duration and the X-ray luminosity in stellar flares. *Proceeding of. Science MULTIF2017*, 060.
- Tsuboi, Y., Yamazaki, K., Sugawara, Y., Kawagoe, A., Kaneto, S., Izuka, R., Matsumura, T., Nakahira, S., Higa, M., Matsuoka, M., Sugizaki, M., Ueda, Y., Kawai, N., Morii, M., Serino, M., Mihara, T., Tomida, H., Ueno, S., Negoro, H., Daikyujii, A., Ebisawa, K., Eguchi, S., Hiroi, K., Ishikawa, M., Isobe, N., Kawasaki, K., Kimura, M., Kitayama, H., Kohama, M., Kotani, T., Nakagawa, Y.E., Nakajima, M., Ozawa, H., Shidatsu, M., Sootome, T., Sugimori, K., Suwa, F., Tsunemi, H., Usui, R., Yamamoto, T., Yamaoka, K., & Yoshida, A., 2016. Large X-ray flares on stars detected with MAXI/GSC: A universal correlation between the duration of a flare and its X-ray luminosity. *arXiv:1609.01925v2*.
- Uchiyama, H., Nobukawa, M., Tsuru Go, T., Koyama, K., 2013. K-Shell Line Distribution of Heavy Elements along the Galactic Plane Observed with Suzaku. *Publication of the Astronomical Society of Japan*. 65, 19.
- Vaiana, G.S., Cassinelli, J.P., Fabbiano, G., Giacconi, R., Golub, L., Gorenstein, P., Haisch, B.M., Harnden Jr., F.R., Johnson, H.M., Linsky, J.L., Maxson, C.W., Mewe, R., Rosner, R., Seward, F., Topka, K., Zwaan, C., 1981. Results from an extensive Einstein stellar survey. *Astrophys J* 245, 163–182. <https://doi.org/10.1086/158797>.
- Van den Oord, G., Mewe, R., 1989. The X-Ray Flare and the Quiescent Emission from Algol as Detected by EXOSAT. *A & A* 213, 245–260.
- Warwick, R.S., 2014. Low-luminosity X-ray sources and the Galactic ridge X-ray emission. *Monthly Notice of the Royal Astronomical Society* 445, 66.
- White, N.E., 1996. Stellar X-ray Spectroscopy with ASCA. *ASP Conference Series* 109, 1996.
- White, N.E., Culhane, J.L., Parmer, A.N., Kellett, B.J., Kahan, S., Van den Oord, G.H.J., Kuuijpers, J., 1986. An EXOSAT observation of quiescent and flare coronal X-ray emission from Algol. *Astrophys J* 301, 262–274.
- White, N., Holt, S., Becker, R., Boldt, E.A., Serlemitsos, P.J., 1980. X-ray Observations of Algol. *Astrophys J* 239, 69–71.
- Xu, Xiao-jie, Wang, Q.D., Li, Xiang-Dong, 2016. Fe Line diagnostic of Cataclysmic variables and Galactic ridge X-ray emission. *Astrophys J* 818:136 (12). <https://doi.org/10.3847/0004-637X/818/2/136>.
- Yamauchi, S., Ebisawa, K., Tanaka, Y., Koyama, K., Matsumoto, H., Yamasaki, N., Takahashi, H., Ezoe, Y., 2009. Iron emission lines on the Galactic ridge observed with Suzaku. *Publication of the Astronomical Society of Japan* 61, 225–232.
- Yang, X., Lu, F., Aschenbach, B., Chen, L., 2011. XMM-Newton Observation of the eclipsing binary Algol. *Res. Astron. Astrophys.* 11 (4), 457–470.
- Yoldas, E., Dal, H.A., 2017. The Chromospherically Active Low-Mass close binary KIC 9761199. *Rev. Mex. Astron. Astrofis.* 53, 67–78.
- Yuasa, T., Makishima, K., Nakazawa, K., 2012. Broadband Spectral analysis of the Galactic ridge X-ray emission. *Astrophys J* 753, 129.
- Yuasa, T., Nakazawa, K., Makishima, K., Saitou, K., Ishida, M., Ebisawa, K., Mori, H., Yamada, S., 2010. White dwarf masses in Intermediate Polars observed with the Suzaku satellite*. *A & A* 520, A25.
- Zavala, R.T., Hummel, C.A., Boboltz, D.A., Ojha, R., Shaffer, D.B., Tycner, C., Richards, M.T., Hutter, D.J., 2010. The Algol triple system spatially resolved at optical wavelengths. *Astrophys. J.*
- Zhang, Li-Yun., Pi, Qing-Feng, & Zhu, Zhong-Zhong, 2015. Chromospheric activity in several single late-type stars*. *Research in Astronomy & Astrophysics* 15 (2), 252–274. [Doi: arxiv.org/abs/1005.0626v1 10.1088/1674-4527/15/2/009](https://doi.org/10.1088/1674-4527/15/2/009).
- Zhao, J.K., Oswalt, T.D., Zhao, G., Lu, Q.H., Luo, A.L., Zhang, L.Y., 2013. Tracers of Chromospheric structure. I. Ca II H & K Emission distribution of 13,000 F, G, and K stars in SDSS DR7 Spectroscopic sample. *The Astronomical Journal* 145 (140).
- Zhao, J. K., Oswalt, T. D., Rudkin, M., Zhao, G., & Chen, Y. Q., 2011. The Chromospheric Activity, Age, Metallicity and Space Motions of 36 Wide Binaries, *The Astronomical Journal* 141: 107. [arxiv:1101.3257v1](https://arxiv.org/abs/1101.3257v1).